



Published in final edited form as:

Osteoarthritis Cartilage. 2017 May ; 25(5): 718–726. doi:10.1016/j.joca.2016.09.007.

Spinal Microglial Activation in a Murine Surgical Model of Knee Osteoarthritis

Phuong B. Tran¹, Rachel E. Miller^{1,2}, Shingo Ishihara¹, Richard J. Miller³, and Anne-Marie Malfait^{1,2,*}

¹Department of Internal Medicine, Division of Rheumatology, Rush University Medical Center, 1611 W. Harrison St, Suite 510, Chicago, IL

²Department of Biochemistry, Rush University Medical Center, 1611 W. Harrison St, Suite 510, Chicago, IL

³Department of Pharmacology, Northwestern University, Chicago, IL

Abstract

Objective—Microgliosis, the activation of microglial cells, is thought to contribute to synaptic transmission in the dorsal horn and thereby promote chronic pain. The primary aim of this study was to document the temporal profile of dorsal horn microgliosis after destabilization of the medial meniscus (DMM) in wild type (WT) and *Adams5* null mice. Since neuronal fractalkine (CX3CL1) contributes to microgliosis, we assessed its release from dorsal root ganglia (DRG) cultures after DMM.

Design—DMM or sham surgery was performed in the right knee of 10-week old male WT, CX3CR1-GFP, or *Adams5* null C57BL/6 mice. Hindpaw mechanical allodynia was monitored using von Frey fibers. L4 dorsal horn microgliosis was assessed 4, 8 and 16 weeks after surgery, based on the morphology of Iba1-immunoreactive microglia. DRG cells (L3-L5) were cultured and supernatants collected for fractalkine ELISA.

Address correspondence to: Anne-Marie Malfait, MD, PhD, Rush University Medical Center, 1611 W Harrison Street, suite 510, 60612 Chicago IL anne-marie_malfait@rush.edu.

Author Contributions

PBT: Conception and design, acquisition of data, analysis and interpretation of data, drafting of the article, and final approval of the article.

REM: Conception and design, acquisition of data, analysis and interpretation of data, critical revision of the article, and final approval of the article.

SI: Acquisition of data, analysis and interpretation of data, and final approval of the article.

RJM: Analysis and interpretation of data, critical revision of the article, and final approval of the article.

AMM: Conception and design, acquisition of data, analysis and interpretation of data, drafting of the article, and final approval of the article.

Anne-Marie Malfait takes responsibility for the integrity of the work as a whole, from inception to finished article.

Conflict of interest

There are no conflicts of interest for any of the authors. AM Malfait serves as an Associate Editor for Osteoarthritis and Cartilage.

Role of the funding source

The funding sources were not involved in the study design, collection, analysis and interpretation of data, or the writing and submission of the manuscript.

Publisher's Disclaimer: This is a PDF file of an unedited manuscript that has been accepted for publication. As a service to our customers we are providing this early version of the manuscript. The manuscript will undergo copyediting, typesetting, and review of the resulting proof before it is published in its final citable form. Please note that during the production process errors may be discovered which could affect the content, and all legal disclaimers that apply to the journal pertain.

Results—In WT mice, numbers of activated microglia were increased 8 and 16 weeks, but not 4 weeks, after DMM but not sham surgery. DRG cultures showed increased basal fractalkine release at 8 and 16 weeks. *Adams5* null mice did not develop mechanical allodynia up to 16 weeks after DMM. Accordingly, DRG cultures from these mice did not exhibit increased fractalkine release and dorsal horn microgliosis did not occur.

Conclusion—DMM surgery leads to late stage dorsal horn microgliosis. The temporal correlation with DRG fractalkine release suggests it may contribute to microgliosis. Reduced microgliosis in *Adams5* null mice, which are protected from joint damage and associated mechanical allodynia after DMM, suggests that microgliosis is associated with joint damage and accompanying persistent pain.

INTRODUCTION

Chronic pain is the major symptom associated with osteoarthritis (OA), and its clinical presentation is complex. Osteoarthritic joint pain has a strong mechanical component, and can be triggered by specific activities such as climbing stairs. As the disease progresses, pain can become more persistent and manifest at rest [1]. Ongoing peripheral input from the affected joint appears to drive the pain, as evidenced by the observation that local joint pain can be abolished by intra-articular anesthetics [2] and - in most cases - by total joint replacement (reviewed in [3]). In the course of OA, nociceptors (specialized sensory neurons that detect potentially harmful stimuli) innervating the affected joint can become sensitized by locally generated products, such as nerve growth factor, inflammatory cytokines and chemokines, prostaglandins [4, 5], and disease-associated molecular patterns (DAMPs) [6] (“peripheral sensitization”). In addition, increased nociceptive input from the periphery heightens activity and excitability in the spinal cord (“central sensitization”) [7]. Thus, OA pain may be driven by abnormal excitability in pain pathways of both the peripheral and central nervous systems (CNS). Indeed, clinical researchers are increasingly reporting signs of sensitization, both peripheral and central, in OA patients. This includes decreased pressure withdrawal thresholds and temporal summation at sites remote from the affected joint [8–11].

Small animal models of OA in rats and mice increasingly incorporate pain related behaviors as outcome measures (reviewed in [12]). The best-characterized model in terms of pain behaviors uses intra-articular injection of the glycolysis inhibitor, mono-iodoacetate (MIA), into the rat or mouse knee in order to kill articular chondrocytes. This causes severe cartilage and subchondral bone damage, and pronounced inflammation [13, 14]. The aggressive joint pathology is accompanied by pain behaviors (reviewed in [15], including mechanical hypersensitivity, weightbearing deficits [13], and ongoing pain [16], all driven both by peripheral and central mechanisms [16–18].

Surgically induced knee OA is also associated with mechanical allodynia, as has been described in the rat medial meniscal tear model [19], after partial meniscectomy in the mouse knee [20], and after destabilization of the medial meniscus (DMM) in the mouse [21–23]. In the latter, mechanical allodynia in the ipsilateral hindpaw develops early after surgery and is maintained for the 16-week follow-up period [21, 22]. Since mechanical allodynia is a

behavioral indicator of sensitization, it is likely that central mechanisms contribute to its development and/or maintenance. It has, however, never been demonstrated whether changes in the spinal cord can be detected in surgical models of OA.

In the current study, we focused on microglial cells in the dorsal horn of the spinal cord, because mounting evidence shows that activation of these cells contributes to the plasticity of synaptic transmission that is associated with chronic pain states [24]. Therefore, the primary aim of this study was to document the temporal profile of microglial activation in the dorsal horn after DMM surgery. Additionally, we assessed fractalkine (FKN, CX3CL1) release by dorsal root ganglia (DRG), because in neuropathic pain models it has been demonstrated that FKN derived from the central terminals of DRG neurons contributes to the activation of dorsal horn microglia, expressing the FKN receptor, CX3CR1 [25–28]. Finally, we explored the role of joint damage in establishing microgliosis, by assessing microglial activation in *Adamts5* null mice. Since *Adamts5* null mice do not develop joint damage or associated mechanical allodynia after DMM surgery [21, 29], we hypothesized that these mice would not develop microgliosis or FKN release purely from the DMM surgery itself.

MATERIALS AND METHODS

Animals

All animal experiments were approved by the Institutional Animal Care and Use Committee at Rush University Medical Center. Animals were housed with food and water *ad libitum* and kept on 12-hour light cycles. We used a total of 107 C57BL/6 mice, including in house wild-types (WT), *Adamts5* null mice [21], and CX3CR1-GFP reporter mice [30]. We used CX3CR1-GFP mice that were heterozygous for the GFP reporter gene.

Surgery

DMM or sham surgery was performed in the right knee of 10-week old male mice, as previously described [31]. Briefly, after medial parapatellar arthrotomy, the anterior fat pad was dissected to expose the anterior medial meniscotibial ligament, which was severed. The knee was flushed with saline and the incision closed. Sham surgery was identical to DMM except that the medial meniscotibial ligament remained intact.

Mechanical allodynia

Mice were tested for sensitivity to von Frey monofilaments, using the up–down staircase method of Dixon [32, 33]. The threshold force required to elicit withdrawal of the paw (median 50% withdrawal) was determined twice on each hind paw (and averaged) on each testing day, with sequential measurements separated by at least 5 min. Baseline thresholds were assessed prior to surgery, and thresholds were assessed 4, 8, 12, and 16 weeks after DMM.

DRG cell culture

Four, 8, or 16 weeks after DMM, ipsilateral and contralateral innervating DRG, L3-L5, were collected and pooled from 4 mice. L3-L5 DRG collected from surgically naïve mice older

than 10 weeks or from sham mice 4 or 8 weeks after surgery were used as controls. Cells were acutely isolated from DRG via collagenase 4 (1 mg/mL) and papain (30 U/mL, Worthington Biochemical Corp, Lakewood, NJ) digestion. Cells were plated on poly-L-lysine and laminin (20 µg/mL) coated glass coverslips within 6-well plate wells, and cultured at 37°C with 5% CO₂ for four days in adult neurogenic medium: F12 with L-glutamine, 0.5% FBS, 1x N2 (Life Technologies), penicillin and streptomycin (100 µg/ml and 100 U/mL). Medium was changed on day 2, and supernatants collected on day 4 for protein analysis. For cell culture experiments, a total of 48 C57BL/6 male mice were used (4 mice pooled per DRG culture in 2 independent experiments). Additionally, 6 *Adams5* null mice (3 DMM and 3 surgically naïve mice in 1 experiment). Each plot shows the result from one independent experiment where each dot represents an individual culture well.

Analysis of basal fractalkine levels in DRG culture supernatants under naïve, sham, and DMM conditions

Cell culture supernatants were concentrated via 3-kDa molecular weight cut-off Millipore Centrifugal Filters (Billerica, MA). Total protein levels were determined by bicinchoninic acid (BCA) assay (Thermo Fisher Scientific, Inc., Rockford, IL). Levels of soluble fractalkine (FKN) were measured via ELISA (R&D Systems Inc, Minneapolis, MN), following manufacturer recommendations.

Immunofluorescence

Mice were anesthetized by ketamine and xylazine and perfused transcardially with PBS followed by 4% paraformaldehyde in PBS [34]. The spinal column was dissected and post fixed overnight in 4% paraformaldehyde followed by cryopreservation in 30% sucrose in PBS. The post fixed spinal column was decalcified in 6% Trichloroacetic acid overnight, followed by cryopreservation in 30% sucrose in PBS [35]. The spinal column was sectioned into corresponding L3-L5 lumbar segments and each segment was embedded in OCT compound, frozen on dry ice and cryosectioned into 20 µm sections [18]. Spinal cord sections were then immunostained with an antibody against ionized calcium-binding adaptor molecule-1 (Iba1) (Wako Chemicals USA, Richmond, VA), followed by a secondary antibody, anti-rabbit conjugated AlexaFluor 488. For CX3CR1-GFP mice, spinal cord sections were immunostained with anti-GFP antibody (Abcam, Cambridge, MA) and anti-Iba1 antibody, followed by the secondary antibodies, anti-chicken conjugated AlexaFluor 488 and anti-rabbit conjugated AlexaFluor 633. As a negative control, spinal cord sections were immunostained with only the secondary antibodies. All images were captured using a laser-scanning confocal microscope and exported to Adobe Photoshop CS5.1 (Adobe, San Jose, CA). Adjustments were made to brightness and contrast to reflect true colors [34]. All images were treated exactly the same in terms of adjustments to brightness and contrast to minimize bias. For immunofluorescence experiments, a total of 38 male WT mice were used for Iba1 staining. Most of the mice within the group came from different litters. In addition, a total of 8 CX3CR1-GFP heterozygous male mice (4 naïve and 4 DMM), and 7 *Adams5* null mice (4 naïve and 3 DMM) were used for spinal cord Iba1 staining.

Assessment of microglial activation

Microglial activation (“microgliosis”) was determined by examining morphology changes in Iba1-immunoreactive (ir) cells, as described [36]. Iba1-ir cells were classified as surveyor (or resting) microglia if their process length was more than double the soma diameter. They were classified as effector (or activated) microglia if their process length was less than double the soma diameter. In a pilot study, we observed that some microgliosis occurred at levels L3-L5 (Supplemental Table 1A–C), but it was most robust at L4, (which is compatible with the findings of Thakur *et al.*, in the rat MIA model) [36]. We therefore also focused on this level for all subsequent experiments and used this level for quantification. In WT and *Adamts5* null mice, activated Iba1-ir microglia were counted in 3 sections per mouse in both ipsilateral and contralateral L4 dorsal horns. The average number of activated microglia for the ipsilateral dorsal horn was comparable to those on the contralateral side and the sums of the counts for both sides were then averaged for each individual mouse. Counts were performed by an observer who was blinded to the experimental groups. In CX3CR1-GFP mice, activated microglia were identified and counted based on GFP expression. In addition to quantification of activated microglia, we also counted the number of resting microglia in the same sections. The total number of microglia was obtained by summing the number of activated and resting microglia.

Histopathology of the knee

Histopathology of the knee was evaluated based on a modified OARSI score [37] (Alison Bendele, Bolder BioPath, Inc., Boulder, CO). Briefly, joints were fixed in 10% formalin for 48 h, and decalcified for 2 days in 10% formic acid. Knee joints were trimmed of extraneous tissue, embedded in the frontal plane and sectioned. One 8- μ m section was taken from each joint at the approximate midpoint of the frontal plane and stained with Toluidine blue. Scoring was performed by an evaluator who was blinded to the experimental groups. Cartilage degeneration and osteophytes were scored using a previously described system [38]. Briefly, cartilage degeneration was scored on the medial femoral condyle and tibial plateau with 0 representing no damage and 30 the maximal score. Osteophytes were measured in the medial compartment by ocular micrometer and scored on a scale of 0 to 3, where 0 represents no osteophytes present.

Statistical analysis

For microglia analyses, non-parametric Mann-Whitney or Kruskal-Wallis tests were used as appropriate. When Kruskal-Wallis tests were significant ($p < 0.05$), *post-hoc* analysis was performed using Dunn's multiple comparisons test. For analysis of protein content, Student's t-test or one-way analysis of variance (ANOVA) was used, as appropriate. When one-way ANOVA results were significant ($p < 0.05$), *post-hoc* analysis was performed using Bonferroni's multiple comparison test. For von Frey testing, one-way ANOVA with Bonferroni post-tests was used to compare each time point to time 0. A p -value < 0.05 was considered significant for all tests. All analyses were carried out using GraphPad Prism version 6.00 for Windows (GraphPad Software, San Diego, CA). Results are presented as mean \pm 95% CI.

RESULTS

Time-course of microglial activation in the dorsal horn

Mechanical sensitivity to von Frey hairs in the ipsilateral hindpaw was monitored up to 16 weeks after DMM surgery and in age-matched naïve controls. As previously reported, we confirmed that the withdrawal threshold was unchanged in naïve mice, while DMM mice developed mechanical allodynia by week 4, which was maintained for the 16-week follow-up period after surgery [6, 38] (data not shown). Four, 8, and 16 weeks after DMM or 8 weeks after sham surgery, we assessed the L4 level of the dorsal horn for Iba1 immunoreactivity, a marker for microglia, and assessed the number of Iba1-ir cells that had an activated morphology (Fig. 1A). Four weeks after DMM, the number of activated microglia was similar to naïve and sham controls (Fig. 1B). In contrast, 8 weeks after DMM surgery, there was a significant increase in the number of activated microglia compared to sham controls. By 16 weeks after DMM, activated microglia were increased compared to sham and age-matched naïve controls. A representative image of the L4 dorsal horn 8 weeks after DMM along with naïve and sham age-matched controls is shown in Fig. 1C, in order to illustrate this. Interestingly, we observed that microgliosis occurred both in the ipsilateral and the contralateral dorsal horn (Fig. 1C), whereas DMM surgery and associated mechanical allodynia are unilateral [21]. When we counted the total number of Iba1-ir cells in the L4 dorsal horn, we detected a trend toward increased numbers of microglial cells in naïve mice with age (Supplemental Fig. 1). Overall, the effect of age was of greater magnitude than the effect of treatment; thus, we observed no differences between naïve, sham, and DMM groups at any given time point.

Microglial activation in the dorsal horn of CX3CR1-GFP reporter mice

CX3CR1 is the G-protein coupled receptor for the chemokine CX3CL1/FKN. In the CNS, CX3CR1 is expressed primarily on microglial cells [26, 27, 39]. To ascertain that this was indeed the case, we performed DMM on CX3CR1-GFP reporter mice ($n=5$), and monitored them for 16 weeks. CX3CR1-GFP reporter mice also developed mechanical allodynia starting 4 weeks after DMM and maintained for the 16-week follow-up period (Supplemental Fig. 2). After 16 weeks, the mice were sacrificed for knee histopathology and for assessment of dorsal horn microgliosis. In terms of joint damage, we found no statistically significant differences between WT and CX3CR1-GFP mice, with a medial cartilage degeneration score of 10 ± 5.95 in WT mice ($n=4$) vs. 9.8 ± 5.85 in CX3CR1-GFP mice ($n=5$), and an osteophyte score of 1.8 ± 0.8 in WT vs. 1.4 ± 1.1 in CX3CR1-GFP mice. Iba1 immunostaining of L4 spinal sections from CX3CR1-GFP reporter mice, either naïve or 16 weeks after DMM, revealed that the vast majority of GFP-expressing cells also expressed Iba1, indicating that CX3CR1 is expressed mainly on microglia, as expected (Fig. 2A). When microglial activation was assessed in CX3CR1-GFP mice by counting GFP-positive cells with an activated phenotype, we observed an increase in the number of activated microglia 16 weeks after DMM compared to naïve controls (Fig. 2B). Thus, we confirmed that the number of activated microglia in CX3CR1-GFP mice (assessed by counting GFP-positive cells with an activated morphology, Fig. 2B) was comparable to that in WT mice 16 weeks after DMM (assessed by counting Iba1-ir cells with an activated morphology, Fig. 1B).

Time-course of soluble FKN release from DRG cultures

FKN, released from the central terminals of nociceptors, has been implicated in driving the activation of dorsal horn microglia [26, 27]. Therefore, we assessed the basal FKN release by DRG cultures prepared 4, 8, or 16 weeks after DMM or sham surgery and from naïve controls (Fig. 2C). The results indicated that 4 weeks after DMM, DRG cells released similar levels of FKN compared to cultures from naïve mice. In contrast, 8 weeks after DMM, DRG cells released increased levels of FKN compared to cultures from naïve or sham-operated mice. Sixteen weeks after DMM, the level of FKN released from DRG cultures was less than 8 weeks after DMM, but still higher than levels produced by DRG cultures 8 weeks after sham surgery and naïve mice.

Adamts5 null mice do not develop microgliosis after DMM surgery

Adamts5 null mice are protected from joint pathology up to 6 months after DMM [29, 40]. We have previously reported that these mice are also protected from mechanical allodynia up to 8 weeks after DMM surgery [21]. Here, we confirmed that *Adamts5* null mice do not develop mechanical allodynia, even up to 16 weeks after DMM (Fig. 3A). Hence, we examined whether the molecular and cellular changes observed after DMM surgery in WT mice are attenuated in *Adamts5* null mice. DRG cultures from *Adamts5* null mice prepared 8 weeks after DMM did not release increased levels of soluble FKN compared to naïve (Fig. 3B). Concordantly, 16 weeks after DMM, *Adamts5* null mice showed no increase in activated microglia compared to age-matched naïve *Adamts5* null mice (Fig. 3C). These results indicate that microglial activation is attenuated in the dorsal horn of *Adamts5* null mice compared to WT mice.

DISCUSSION

In this study, we have demonstrated that spinal microgliosis is a feature of late-stage experimental OA after DMM surgery. Sensory nociceptive neurons are the essential mediators of pain, but for the genesis of chronic pain, neuronal interactions with glial cells are also crucially important [24, 41]. In particular, activated microglial cells have been shown to promote chronic pain states through the production of pro-inflammatory cytokines, chemokines, and extracellular proteases [41, 42]. Microglial cells are the resident macrophages of the CNS and their activation has been extensively documented in rodent models of neuropathic and inflammatory pain. For example, peripheral nerve injury (PNI) causes microglial activation in the spinal cord [43], which contributes to pathogenesis of neuropathic pain (reviewed in [44]). The extent and the temporal profile of microglial activation varies among models [44], but typically microgliosis has a rapid onset: the first signs can appear within 24 hours after PNI, when the somata of microglial cells become hypertrophic and the thin processes withdraw [45]. At this time microglial cells are also seen to proliferate [46]. Inflammation in peripheral tissues is also accompanied by microgliosis that can occur acutely after intraplantar or intra-articular injection of complete Freund's adjuvant (CFA), which results in pain-related behavioral hypersensitivity and microgliosis within hours [47, 48]. Only recently have researchers started to explore microglial activation associated with experimental OA, using the MIA model. In a rat study, 2 mg MIA injected into the knee resulted in secondary allodynia as early as day 3, and was maintained for the

14-day follow-up period. Furthermore, microgliosis was present from day 3 through day 14, peaking at day 7 [36]. In a mouse study, 1 mg MIA injected into the knee joint caused secondary allodynia by day 3, and was maintained for 28 days. At both time points, the number of dorsal horn Iba1-ir microglia was enhanced in MIA compared with saline controls, although this increase reached statistical significance only at 28 days [18]. Thus, in the MIA model, microgliosis developed quite rapidly but was most prominent in later stages, indicating that it may contribute to the persistence of OA-related pain.

The rapidly progressive joint pathology after MIA injection [13, 14] may obscure the fine temporal relationships between joint changes and pathological processes in the pain pathway. In contrast, joint damage after DMM surgery progresses very slowly: during the first 8 weeks, cartilage degeneration and osteophyte formation are mild to moderate, while joint damage accelerates between weeks 8 and 16 [38, 49]. Concomitantly with progressive joint damage, DMM mice develop progressive mechanical allodynia [21, 23], which appears 4 weeks after surgery and is maintained for 16 weeks, whereas sham surgery results in a short-lived mechanical allodynia at 4 weeks [22]. Further, it has been shown that weightbearing deficits [50] and locomotor changes indicative of pain [22, 50] do not appear until after 8 weeks *post* DMM but not sham surgery. Therefore, the temporal profile of pain related behaviors after DMM suggests that pain in this model develops in two stages: an early stage, up to week 8, and a late stage between weeks 8 and 16 [22, 50]. Indeed, we have previously reported that the 8-week time point may be crucial, with L3-L5 DRG cells showing increased expression of the proalgesic chemokine, MCP-1, and its receptor, CCR2, which provide a key signaling pathway for the persistence of pain after week 8 [22].

To the best of our knowledge, this is the first report of microglial changes in a surgical model of OA. Interestingly, microgliosis started 8 weeks after DMM, and not sham, surgery and was firmly established by week 16. Thus, the temporal correlation of microglial activation in the dorsal horn to the pain behaviors exhibited 8 and 16 weeks after DMM suggests that microgliosis may be involved in the maintenance of OA pain.

Furthermore, we found that mice lacking *Adams5*, which are protected from joint damage and mechanical allodynia after DMM [21, 29], did not display microgliosis. Absence of microglial activation in these mice suggests that protecting the joint and preventing peripheral sensitization can attenuate aspects of central sensitization and that OA joint damage can trigger molecular and cellular changes in the nociceptive pathway. However, an alternative explanation might be that ADAMTS-5 plays a direct role in the nervous system, and it has indeed been shown that DRG neurons can express this enzyme [51, 52], although information on a biological role of neuronal ADAMTS-5 in pain is not yet available.

It is noteworthy that the total numbers of Iba1-ir in the dorsal horn were not significantly different between naïve, sham, and DMM-operated WT mice at any time point, but we found a trend for increased total numbers of Iba1-ir cells with age. This trend has also been reported in other studies, where the total number of microglia has been shown to significantly increase with age in various regions in the CNS, including the spinal cord [53]. The significance of increasing microglial number with age is currently unclear, although one hypothesis suggests that it may be a compensatory mechanism to maintain overall function

[54]. This observation underscores the need for including age-matched controls when performing long term *in vivo* studies such as here.

FKN is a unique chemokine in that it has been reported to be attached to the membranes of DRG cell bodies [26, 55], primary afferent fibers [26], as well as spinal neurons [26, 28], although expression of FKN in sensory neurons *in vivo* has not been definitively demonstrated. FKN must be cleaved from the membrane into a soluble fragment in order to activate its receptor on spinal microglia [27]. Several proteases may be involved in FKN cleavage, including cathepsin S, ADAM-10, and ADAM-17 [27]. In models of neuropathic pain, it has been clearly demonstrated that FKN derived from the central terminals of DRG neurons is critically involved in establishing chronic pain and is associated with the activation of CX3CR1-expressing microglia in the spinal cord [25, 26, 28]. FKN can cause microglia activation, as evidenced by elevated intracellular calcium, activation of mitogen activated protein kinases, as well as activation of protein kinase B/Akt and actin rearrangement [56–58]. A role for neuronal FKN in microglia activation has also been demonstrated in models of acute peripheral inflammation. In a rat monoarthritis model, intra-articular injection of CFA produced robust microglia activation and increased expression of neuronal FKN in the spinal cord [48]. Here, the use of CX3CR1-GFP reporter mice confirmed that the FKN receptor was expressed primarily on microglia. Hence, we decided to evaluate release of FKN by cultured DRG neurons at several intervals after DMM and found that FKN release was not increased 4 weeks after DMM, but was strongly increased 8 weeks and to a lesser degree 16 weeks after DMM. The temporal correlation of FKN release with microglial activation suggests that FKN may contribute to spinal microglial activation in the dorsal horn in this model. This is further supported by the observation that DRG cultures from *Adams5* null mice, which do not display microgliosis 16 weeks after DMM, did not secrete increased levels of soluble FKN.

The current study extends our previous report on the biphasic nature of pain-related behaviors in association with progressive experimental OA after DMM [22]. As in other chronic pain models, we observed an interesting correlation between the development of microglial activation and pain behavior. It should be noted, however, that our observations on microglial activation or measurements of FKN release do not demonstrate that these changes actually cause the observed pain related behaviors. Although such changes support many current ideas on the mechanisms by which chronic pain is produced, it is not clear which aspects of pain behavior they explain. For example, we observed that changes in microglial activation occur bilaterally. There is a growing body of evidence that unilateral models that are associated with unilateral allodynia (either inflammatory/arthritis models such as the zymosan model or IA injection of MIA, or nerve injury models) provoke bilateral changes in the nervous system, both in the DRG (macrophage infiltration, molecular changes) and in the CNS (microgliosis, molecular changes) [55, 59, 60]. This phenomenon is not at all well understood, and it suggests that peripheral injury may lead to more generalized neuroinflammatory changes in the peripheral and central nervous system. It is potentially important to be aware of this phenomenon in the context of OA, although its significance is at this time not clear. Further, it should be considered that activated microglia can also exert a protective effect on chronic pain [61]. Therefore, understanding the biological significance of the observed microgliosis in this experimental model of OA and

associated pain-related behaviors will require in depth characterization of the activated microglia as well as interventional studies to modulate microglia.

While these are clear limitations of the study, we do think that our observations contribute novel insights into the development of OA-associated pain and may pave the way for more mechanistic studies to explore the role of central sensitization in chronic OA pain. We propose that careful longitudinal dissection/analysis of pain pathways will contribute to our understanding of how pain signals propagate from the periphery to the central nervous system in OA, and allow for differential testing of targeted intervention in early vs. late stage OA.

Supplementary Material

Refer to Web version on PubMed Central for supplementary material.

Acknowledgments

This work was supported by National Institutes of Health/National Institute of Arthritis and Musculoskeletal and Skin Diseases (NIAMS) grants R01-AR-064251 and R01-AR-060364. Dr. R.E. Miller was supported by NIAMS grant F32-AR-062927 and an Arthritis Foundation Postdoctoral Fellowship Grant.

References

1. Hawker GA, Stewart L, French MR, Cibere J, Jordan JM, March L, et al. Understanding the pain experience in hip and knee osteoarthritis--an OARSI/OMERACT initiative. *Osteoarthritis Cartilage*. 2008; 16:415–422. [PubMed: 18296075]
2. Creamer P, Hunt M, Dieppe P. Pain mechanisms in osteoarthritis of the knee: effect of intraarticular anesthetic. *J Rheumatol*. 1996; 23:1031–1036. [PubMed: 8782136]
3. Malfait AM, Schnitzer TJ. Towards a mechanism-based approach to pain management in osteoarthritis. *Nat Rev Rheumatol*. 2013; 9:654–664. [PubMed: 24045707]
4. Krustev E, Rioux D, McDougall JJ. Mechanisms and Mediators That Drive Arthritis Pain. *Curr Osteoporos Rep*. 2015; 13:216–224. [PubMed: 26025232]
5. Miller RE, Miller RJ, Malfait AM. Osteoarthritis joint pain: the cytokine connection. *Cytokine*. 2014; 70:185–193. [PubMed: 25066335]
6. Miller RE, Belmadani A, Ishihara S, Tran PB, Ren D, Miller RJ, et al. Damage-Associated Molecular Patterns Generated in Osteoarthritis Directly Excite Murine Nociceptive Neurons Through Toll-like Receptor 4. *Arthritis Rheumatol*. 2015; 67:2933–2943. [PubMed: 26245312]
7. Woolf CJ. Central sensitization: implications for the diagnosis and treatment of pain. *Pain*. 2011; 152:S2–15. [PubMed: 20961685]
8. Hassan H, Walsh DA. Central pain processing in osteoarthritis: implications for treatment. *Pain Manag*. 2014; 4:45–56. [PubMed: 24641343]
9. Mease PJ, Hanna S, Frakes EP, Altman RD. Pain mechanisms in osteoarthritis: understanding the role of central pain and current approaches to its treatment. *J Rheumatol*. 2011; 38:1546–1551. [PubMed: 21632678]
10. Neogi T, Guermazi A, Roemer F, Nevitt M, Scholz J, Arendt-Nielsen L, et al. Joint inflammation is associated with pain sensitization in knee osteoarthritis: The Multicenter Osteoarthritis Study. *Arthritis Rheumatol*. 2015
11. Suokas AK, Walsh DA, McWilliams DF, Condon L, Moreton B, Wylde V, et al. Quantitative sensory testing in painful osteoarthritis: a systematic review and meta-analysis. *Osteoarthritis Cartilage*. 2012; 20:1075–1085. [PubMed: 22796624]
12. Malfait AM, Little CB. On the predictive utility of animal models of osteoarthritis. *Arthritis Res Ther*. 2015; 17:225. [PubMed: 26364707]

13. Clements KM, Ball AD, Jones HB, Brinckmann S, Read SJ, Murray F. Cellular and histopathological changes in the infrapatellar fat pad in the monoiodoacetate model of osteoarthritis pain. *Osteoarthritis Cartilage*. 2009; 17:805–812. [PubMed: 19114312]
14. Guzman RE, Evans MG, Bove S, Morenko B, Kilgore K. Mono-iodoacetate-induced histologic changes in subchondral bone and articular cartilage of rat femorotibial joints: an animal model of osteoarthritis. *Toxicol Pathol*. 2003; 31:619–624. [PubMed: 14585729]
15. Malfait AM, Little CB, McDougall JJ. A commentary on modelling osteoarthritis pain in small animals. *Osteoarthritis Cartilage*. 2013; 21:1316–1326. [PubMed: 23973146]
16. Okun A, Liu P, Davis P, Ren J, Remeniuk B, Brion T, et al. Afferent drive elicits ongoing pain in a model of advanced osteoarthritis. *Pain*. 2012; 153:924–933. [PubMed: 22387095]
17. Harvey VL, Dickenson AH. Behavioural and electrophysiological characterisation of experimentally induced osteoarthritis and neuropathy in C57Bl/6 mice. *Mol Pain*. 2009; 5:18. [PubMed: 19379487]
18. Ogbonna AC, Clark AK, Gentry C, Hobbs C, Malcangio M. Pain-like behaviour and spinal changes in the monosodium iodoacetate model of osteoarthritis in C57Bl/6 mice. *Eur J Pain*. 2013; 17:514–526. [PubMed: 23169679]
19. Bove SE, Laemont KD, Brooker RM, Osborn MN, Sanchez BM, Guzman RE, et al. Surgically induced osteoarthritis in the rat results in the development of both osteoarthritis-like joint pain and secondary hyperalgesia. *Osteoarthritis Cartilage*. 2006; 14:1041–1048. [PubMed: 16769229]
20. Knights CB, Gentry C, Bevan S. Partial medial meniscectomy produces osteoarthritis pain-related behaviour in female C57BL/6 mice. *Pain*. 2012; 153:281–292. [PubMed: 22001658]
21. Malfait AM, Ritchie J, Gil AS, Austin JS, Hartke J, Qin W, et al. ADAMTS-5 deficient mice do not develop mechanical allodynia associated with osteoarthritis following medial meniscal destabilization. *Osteoarthritis Cartilage*. 2010; 18:572–580. [PubMed: 20036347]
22. Miller RE, Tran PB, Das R, Ghoreishi-Haack N, Ren D, Miller RJ, et al. CCR2 chemokine receptor signaling mediates pain in experimental osteoarthritis. *Proc Natl Acad Sci U S A*. 2012; 109:20602–20607. [PubMed: 23185004]
23. Kamath RV, Simler G, Zhou C, Hart M, Joshi S, Honore P. Development and validation of mechanical allodynia as a pain readout in a preclinical model of osteoarthritis. *Osteoarthritis Cartilage*. 2012; 20:S62.
24. Taves S, Berta T, Chen G, Ji RR. Microglia and spinal cord synaptic plasticity in persistent pain. *Neural Plast*. 2013; 2013:753656. [PubMed: 24024042]
25. Old EA, Clark AK, Malcangio M. The role of glia in the spinal cord in neuropathic and inflammatory pain. *Handb Exp Pharmacol*. 2015; 227:145–170. [PubMed: 25846618]
26. Verge GM, Milligan ED, Maier SF, Watkins LR, Naeve GS, Foster AC. Fractalkine (CX3CL1) and fractalkine receptor (CX3CR1) distribution in spinal cord and dorsal root ganglia under basal and neuropathic pain conditions. *Eur J Neurosci*. 2004; 20:1150–1160. [PubMed: 15341587]
27. Clark AK, Malcangio M. Fractalkine/CX3CR1 signaling during neuropathic pain. *Front Cell Neurosci*. 2014; 8:121. [PubMed: 24847207]
28. Clark AK, Yip PK, Malcangio M. The liberation of fractalkine in the dorsal horn requires microglial cathepsin S. *J Neurosci*. 2009; 29:6945–6954. [PubMed: 19474321]
29. Glasson SS, Askew R, Sheppard B, Carito B, Blanchet T, Ma HL, et al. Deletion of active ADAMTS5 prevents cartilage degradation in a murine model of osteoarthritis. *Nature*. 2005; 434:644–648. [PubMed: 15800624]
30. Abraham J, Fox PD, Condello C, Bartolini A, Koh S. Minocycline attenuates microglia activation and blocks the long-term epileptogenic effects of early-life seizures. *Neurobiol Dis*. 2012; 46:425–430. [PubMed: 22366182]
31. Glasson SS, Blanchet TJ, Morris EA. The surgical destabilization of the medial meniscus (DMM) model of osteoarthritis in the 129/SvEv mouse. *Osteoarthritis Cartilage*. 2007; 15:1061–1069. [PubMed: 17470400]
32. Chaplan SR, Bach FW, Pogrel JW, Chung JM, Yaksh TL. Quantitative assessment of tactile allodynia in the rat paw. *J Neurosci Methods*. 1994; 53:55–63. [PubMed: 7990513]
33. Dixon WJ. Efficient analysis of experimental observations. *Annu Rev Pharmacol Toxicol*. 1980; 20:441–462. [PubMed: 7387124]

34. Tran PB, Banisadr G, Ren D, Chenn A, Miller RJ. Chemokine receptor expression by neural progenitor cells in neurogenic regions of mouse brain. *J Comp Neurol.* 2007; 500:1007–1033. [PubMed: 17183554]
35. Begum F, Zhu W, Namaka MP, Frost EE. A novel decalcification method for adult rodent bone for histological analysis of peripheral-central nervous system connections. *J Neurosci Methods.* 2010; 187:59–66. [PubMed: 20043948]
36. Thakur M, Rahman W, Hobbs C, Dickenson AH, Bennett DL. Characterisation of a peripheral neuropathic component of the rat monoiodoacetate model of osteoarthritis. *PLoS One.* 2012; 7:e33730. [PubMed: 22470467]
37. Glasson SS, Chambers MG, Van Den Berg WB, Little CB. The OARSI histopathology initiative – recommendations for histological assessments of osteoarthritis in the mouse. *Osteoarthritis Cartilage.* 2010; 18(Suppl 3):S17– 23.
38. Miller RE, Tran PB, Ishihara S, Larkin J, Malfait AM. Therapeutic effects of an anti-ADAMTS-5 antibody on joint damage and mechanical allodynia in a murine model of osteoarthritis. *Osteoarthritis Cartilage.* 2015
39. Wolf Y, Yona S, Kim KW, Jung S. Microglia, seen from the CX3CR1 angle. *Front Cell Neurosci.* 2013; 7:26. [PubMed: 23507975]
40. Glasson, SS., Hopkins, B., Attipoe, S., Schelling, S., Morris, EA. ADAMS-5 KO mice are protected in a long-term instability model of osteoarthritis. 53rd Annual Meeting of the Orthopaedic Research Society; San Diego, CA. Feb 11–14, 2007;
41. Schomburg D, Olson JK. Immune responses of microglia in the spinal cord: contribution to pain states. *Exp Neurol.* 2012; 234:262–270. [PubMed: 22226600]
42. O'Callaghan JP, Miller DB. Spinal glia and chronic pain. *Metabolism.* 2010; 59(Suppl 1):S21–26. [PubMed: 20837189]
43. Watkins LR, Milligan ED, Maier SF. Spinal cord glia: new players in pain. *Pain.* 2001; 93:201–205. [PubMed: 11514078]
44. Tsuda M, Inoue K, Salter MW. Neuropathic pain and spinal microglia: a big problem from molecules in "small" glia. *Trends Neurosci.* 2005; 28:101–107. [PubMed: 15667933]
45. Eriksson NP, Persson JK, Svensson M, Arvidsson J, Molander C, Aldskogius H. A quantitative analysis of the microglial cell reaction in central primary sensory projection territories following peripheral nerve injury in the adult rat. *Exp Brain Res.* 1993; 96:19–27. [PubMed: 8243580]
46. Gehrmann J, Banati RB. Microglial turnover in the injured CNS: activated microglia undergo delayed DNA fragmentation following peripheral nerve injury. *J Neuropathol Exp Neurol.* 1995; 54:680–688. [PubMed: 7666057]
47. Raghavendra V, Tanga FY, DeLeo JA. Complete Freund's adjuvant-induced peripheral inflammation evokes glial activation and proinflammatory cytokine expression in the CNS. *Eur J Neurosci.* 2004; 20:467–473. [PubMed: 15233755]
48. Yang JL, Xu B, Li SS, Zhang WS, Xu H, Deng XM, et al. Gabapentin reduces CX3CL1 signaling and blocks spinal microglial activation in monoarthritic rats. *Mol Brain.* 2012; 5:18. [PubMed: 22647647]
49. Jackson MT, Moradi B, Zaki S, Smith MM, McCracken S, Smith SM, et al. Depletion of protease-activated receptor 2 but not protease-activated receptor 1 may confer protection against osteoarthritis in mice through extracartilaginous mechanisms. *Arthritis Rheumatol.* 2014; 66:3337–3348. [PubMed: 25200274]
50. Inglis JJ, McNamee KE, Chia SL, Essex D, Feldmann M, Williams RO, et al. Regulation of pain sensitivity in experimental osteoarthritis by the endogenous peripheral opioid system. *Arthritis Rheum.* 2008; 58:3110–3119. [PubMed: 18821665]
51. McCulloch DR, Le Goff C, Bhatt S, Dixon LJ, Sandy JD, Apte SS. Adamts5, the gene encoding a proteoglycan-degrading metalloprotease, is expressed by specific cell lineages during mouse embryonic development and in adult tissues. *Gene Expr Patterns.* 2009; 9:314–323. [PubMed: 19250981]
52. Reinhold AK, Batti L, Bilbao D, Buness A, Rittner HL, Heppenstall PA. Differential transcriptional profiling of damaged and intact adjacent dorsal root ganglia neurons in neuropathic pain. *PLoS One.* 2015; 10:e0123342. [PubMed: 25880204]

53. Lee S, Wu Y, Shi XQ, Zhang J. Characteristics of spinal microglia in aged and obese mice: potential contributions to impaired sensory behavior. *Immun Ageing*. 2015; 12:22. [PubMed: 26604973]
54. Wong WT. Microglial aging in the healthy CNS: phenotypes, drivers, and rejuvenation. *Front Cell Neurosci*. 2013; 7:22. [PubMed: 23493481]
55. Clark AK, Gentry C, Bradbury EJ, McMahon SB, Malcangio M. Role of spinal microglia in rat models of peripheral nerve injury and inflammation. *Eur J Pain*. 2007; 11:223–230. [PubMed: 16545974]
56. Chapman GA, Moores K, Harrison D, Campbell CA, Stewart BR, Strijbos PJ. Fractalkine cleavage from neuronal membranes represents an acute event in the inflammatory response to excitotoxic brain damage. *J Neurosci*. 2000; 20:RC87. [PubMed: 10899174]
57. Harrison JK, Jiang Y, Chen S, Xia Y, Maciejewski D, McNamara RK, et al. Role for neuronally derived fractalkine in mediating interactions between neurons and CX3CR1-expressing microglia. *Proc Natl Acad Sci U S A*. 1998; 95:10896–10901. [PubMed: 9724801]
58. Maciejewski-Lenoir D, Chen S, Feng L, Maki R, Bacon KB. Characterization of fractalkine in rat brain cells: migratory and activation signals for CX3CR1-expressing microglia. *J Immunol*. 1999; 163:1628–1635. [PubMed: 10415068]
59. Jancialek R, Dubovy P, Svizenska I, Klusakova I. Bilateral changes of TNF-alpha and IL-10 protein in the lumbar and cervical dorsal root ganglia following a unilateral chronic constriction injury of the sciatic nerve. *J Neuroinflammation*. 2010; 7:11. [PubMed: 20146792]
60. Sagar DR, Stanciaszek LE, Okine BN, Woodhams S, Norris LM, Pearson RG, et al. Tonic modulation of spinal hyperexcitability by the endocannabinoid receptor system in a rat model of osteoarthritis pain. *Arthritis Rheum*. 2010; 62:3666–3676. [PubMed: 20722027]
61. Milligan ER, Watkins L. Pathological and protective roles of glia in chronic pain. *Nat Rev Neurosci*. 2009; 10:23–36. [PubMed: 19096368]

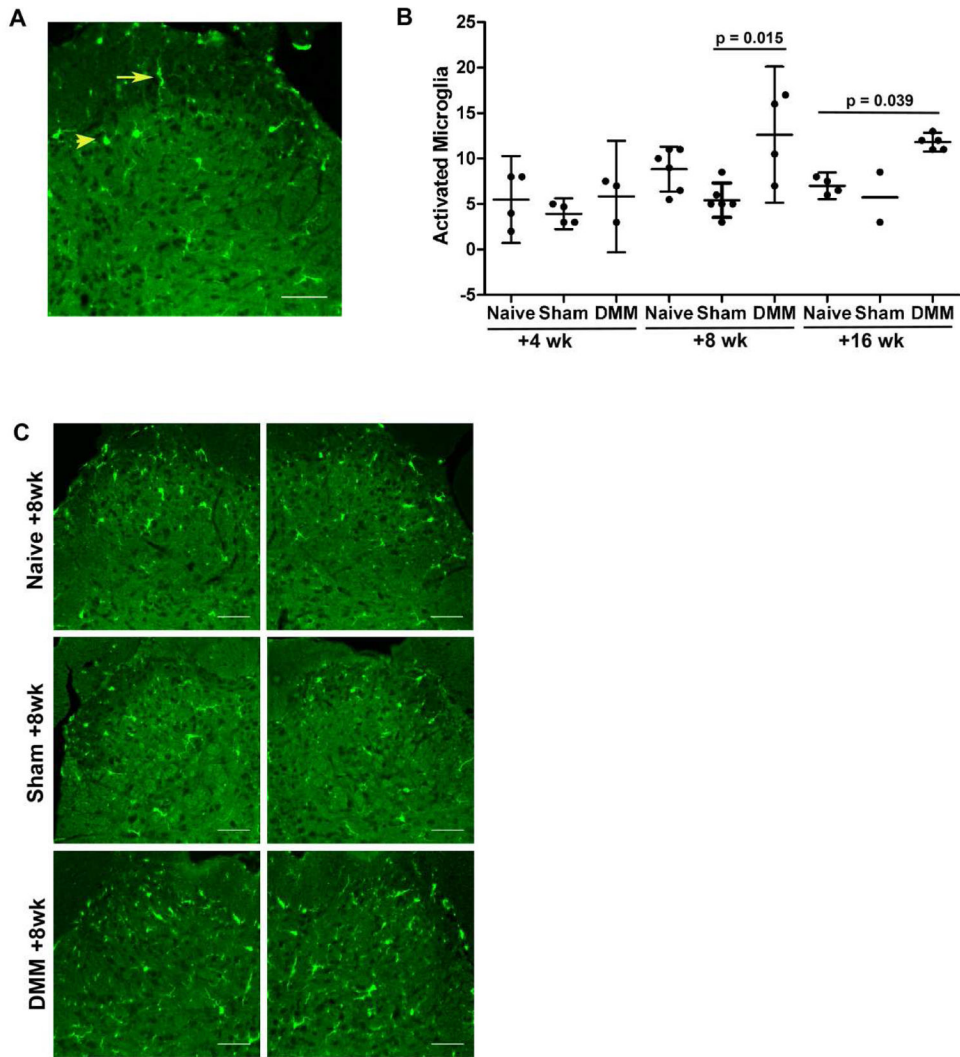


Fig 1. **A)** Representative image of the L4 dorsal horn demonstrating morphological differences between resting (arrow) and activated (arrow head) microglia; **B)** Numbers of activated microglia were counted in the ipsilateral and contralateral L4 dorsal horn of C57BL/6 DMM mice 4, 8 and 16 weeks after surgery along with age-matched naïve and sham controls. Each dot represents the average count of 3 sections per mouse. mean ± 95% CI; **C)** Representative images of Iba1 immunostaining in ipsilateral and contralateral L4 dorsal horns from C57BL/6 DMM mice 8 weeks after surgery along with naïve and sham age-matched controls. Scale bar = 50 µm.

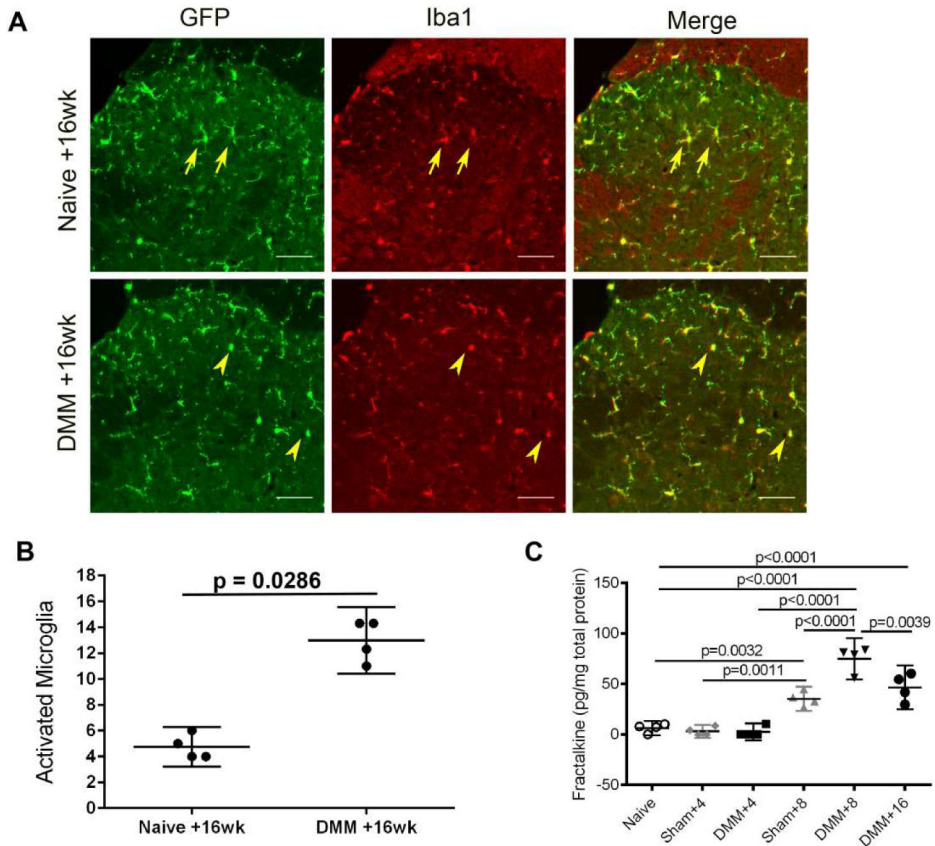


Fig 2. A) Representative images of GFP and Iba1 immunostaining in ipsilateral L4 dorsal horns from age-matched CX3CR1-GFP^{+/-} mice, naïve or 16 weeks after DMM surgery. Arrows indicate resting microglia and arrowheads indicate activated microglia. The merged image shows co-localization of GFP and Iba1. Scale bar = 50 µm; **B**) Numbers of activated microglia (based on GFP immunostaining) were counted in the ipsilateral and contralateral L4 dorsal horn 16 weeks after DMM and in naïve control CX3CR1-GFP^{+/-} mice. Each dot represents the mean count of 3 sections for one mouse; **C**) Four, eight, or sixteen weeks after surgery, DRG cells were cultured from WT C57BL/6 naïve, sham, or DMM mice, and supernatants were analyzed for fractalkine protein. Mean ± 95% CI. Dots represent individual culture wells. Plot shows the result of one out of two independent experiments.

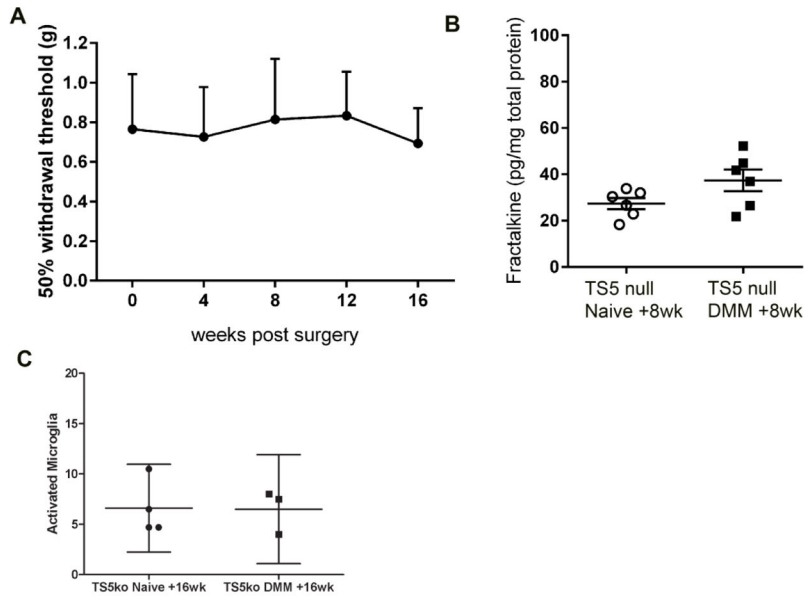


Fig 3. A) Mechanical allodynia was assessed in the ipsilateral hind paw of *Adamts5* null mice (n=5) through 16 weeks after DMM surgery. No statistical differences from time 0 were detected; B) DRG cells were cultured from *Adamts5* null mice, naïve or 8 weeks after DMM, and supernatants were analyzed for fractalkine protein. Dots represent individual culture wells. p=0.09; C) Numbers of activated microglia were counted in the ipsilateral and contralateral L4 dorsal horn 16 weeks after DMM and in naïve control *Adamts5* null mice. Each dot represents the mean count of 3 sections for one mouse. mean ± 95%CI.